PETROPHYSICS, VOL. 53, NO. 4 (AUGUST 2012); PAGE 256–271; 12 FIGURES; 2 TABLES

NEW METHOD FOR PREDICTING PROPERTIES OF LIVE OILS FROM NMR[1]

Vivek Anand[2] and Robert Freedman[2]

ABSTRACT

Crude oil properties such as viscosity, molecular composition, and saturate, aromatic, resin, and asphaltene (SARA) fractions are crucial parameters for evaluating reservoir quality, producibility, and compartmentalization. In the past, physical and empirical models that relate oil properties to NMR measurements have been developed. However, the existing models are too simplistic to accurately predict properties of crude oils which are complex mixtures of hydrocarbon and non-hydrocarbon molecules.

This paper introduces a model-independent technique for quantitative predictions of live-oil properties from NMR measurements. The technique assumes that the physics connecting NMR measurements to oil properties is implicitly contained within a database of NMR and fluid-property measurements made on a representative suite of live oils. The input measurements are mapped to oil properties using a mapping function that is a linear combination of Gaussian radial basis functions. The parameters of the mapping function are determined from the database. The mapping function predicts properties from input measurements made on live oils that are not in the database.

To validate the technique, an extensive database of NMR and fluid-property measurements made on live oils at elevated temperatures and pressures was acquired. Viscosities, molecular compositions, and SARA fractions were accurately determined from NMR measurements using the mapping function technique.

INTRODUCTION

Characterization of reservoir fluids is crucial for several aspects of reservoir development and management. Fluid properties such as viscosity and molecular composition are used for calculation of flow rates and sweep efficiencies of secondary and tertiary recoveries. Gas-oil ratio (GOR) of reservoir fluids is an important parameter for material selection of well completion and design of surface facilities. Asphaltene and wax concentrations are key considerations for flow assurance in completions, pipelines, and surface facilities. Estimation of fluid properties at different depths in a reservoir provides indications of compositional grading and compartmentalization within the reservoir (Elshahawi et al., 2004; Okuyig et al., 2007; Ratulowski et al., 2004). The direct measurement of fluid properties in laboratory is, however, time consuming and expensive. As a result, it is useful to estimate fluid properties from measurements such as NMR, which can be performed with relative ease and at downhole temperature and pressure conditions.

NMR response of fluids provides a link between microscopic molecular motions and macroscopic properties such as viscosity and composition. The relationship between viscosity and relaxation time of pure fluids was established by the phenomenological relaxation theory of Bloembergen, Purcell and Pound (1948) referred to as the BPP theory. Brown (1961) studied proton relaxation in a suite of crude oils with various compositions and viscosities. The viscosities of the samples varied from about 0.5 to 400 cp. He found that the relaxation times showed an inverse dependence on viscosity over the entire range. Since the early work of Brown, several physical and empirical models have been proposed that relate crude oil properties to NMR response. However, the predictive power of these models is limited for several reasons. First, crude oils are complex mixtures of linear, branched, cyclic, and aromatic hydrocarbons. They also contain compounds with sulfur, oxygen, and nitrogen atoms in addition to small concentrations of metals such as nickel and vanadium. As a result, NMR response of crude oils is governed by a multitude of intra- and inter-

Manuscript received by the Editor April 2011; revised manuscript received August 16, 2012.
[1]Originally presented at the SPWLA 50th Annual Logging Symposium, The Woodlands, TX, USA, June 21–24, 2009, Paper AAAA.
[2]Schlumberger, 110 Schlumberger Drive, Sugar Land, TX 77478, USA; Email: vanand@slb.com, freedman1@slb.com.

molecular interactions between the constituents. It is difficult to accurately describe all such interactions by simple physical or empirical models. Second, the detailed information contained in the shapes of T_1 or T_2 distributions is generally not used in the models. Last, the empirical constants involved in the models are not universal, and may differ by as much as a factor of two for different oils.

This paper provides a new model-independent technique for quantitative prediction of live-oil properties from NMR measurements. The basis of the proposed technique is the assumption that there exists a deterministic and unique relationship between NMR response and live-oil properties. This relationship, although not known in closed functional form, is sufficiently contained in a database of NMR and fluid-property measurements made on a suite of live oils. The technique proposes that the relationship can be approximated by a multivariate function that maps the NMR measurements to the fluid properties. The mapping function is a linear combination of Gaussian radial basis functions (RBFs). The coefficients of the mapping function are uniquely determined from the database measurements such that the NMR measurements for each live oil in the database are exactly mapped to the corresponding fluid properties. For a live-oil sample not included in the database, a prediction of the fluid-property is obtained from NMR measurements made on this oil using the mapping function. Such a prediction is thus consistent with the database measurements. If the database is sufficiently populated with representative live-oil samples, the proposed technique is capable of providing accurate predictions. The domain of validity of the mapping function is the range of fluid properties and measurement conditions (temperature and pressure) included in the database. For example, consider a database used to construct a mapping function for predicting viscosity of live oils from NMR measurements. Suppose that the database contains measurements on oils with viscosity between 0.1 and 100 cp. Then the mapping function can be used to accurately predict oil viscosity in the range from 0.1 to 100 cp; however the predictions will not be accurate for viscosities significantly outside this range.

The proposed technique offers several advantages over the conventional approach based on empirical or physical models. First, it is not required to construct an approximate equation or model to relate NMR measurements to live oil properties. The mapping function is general, easy to construct and can accurately represent any continuous nonlinear functional relationship. Once the mapping function is constructed, there are no unknown empirical parameters that need to be adjusted. Another advantage of this technique is that that it is easy to incorporate many different types of auxiliary measurements as inputs including those described by vectors or distributions. Therefore, the detailed information contained in the shapes of NMR distributions is applied to provide accurate predictions of fluid properties.

The mapping function technique also offers several advantages compared to other database approaches such as Artificial Neural Networks (ANN) (Haykin, 1999). For instance, implementation of ANN requires computationally expensive and lengthy iterative training which may not converge to a solution. In contrast, the present approach is a single-shot method that requires no iterative training. The mathematical properties of RBF mapping ensure that a unique solution always exists. Additionally, this technique requires a smaller database for accurate predictions compared to most ANN based methods. The technique is applicable to a wide variety of complex petrophysical problems for which a database of measurements is available (Freedman, 2006). Anand et al. (2011) used the mapping technique to predict effective permeability to oil in sandstones and carbonates from well-log data. Gao et al. (2011) applied the technique to predict capillary pressure curves in complex carbonate rocks from NMR T_2 distributions. Recently, Freedman et al. (2012) described another application of the technique for accurate prediction of formation-thermal-neutron capture cross sections from well-logging data.

The paper is organized as follows. In the second section, a detailed mathematical background for the mapping function technique is provided. The third section describes the database of NMR and fluid-property measurements made on live crude oils. The fourth section illustrates the application of the proposed technique for prediction of viscosities, molecular compositions, and saturate, aromatic, resin, and asphaltene (SARA) fractions of live oils using the laboratory database. The last section discusses the effect of measurement noise on the accuracy of the predictions.

RADIAL BASIS FUNCTION MAPPING

Radial basis functions (RBF) are used for several applications in numerical and scientific computing such as solution of partial differential equations, ANNs, surface reconstruction, computer-aided design (CAD), computer graphics, and multivariate interpolation. A unique property of RBFs is that they provide excellent interpolants for high-dimensionality data sets of poorly distributed data points. This property follows from the mathematical result that the linear system of interpolation equations with RBFs is invertible under very mild conditions. The theoretical background for the invertibility of the RBF interpolation matrix was established in a seminal paper by Micchelli (1986). Franke (1982) published a survey paper on the evaluation of 29 interpolating methods, and concluded that the interpolation by multiquadric RBFs outperformed most methods. The application of RBFs for numerical solution of elliptic, hyperbolic, and parabolic differential equations was developed by Kansa (1990). Since Kansa's work, RBFs are extensively used for approximating scattered, non-uniformly distributed data.

The traditional approach for solving an inverse problem involves fitting a theoretical or empirical model to measurements (Tarantola, 2005). This approach is, in general, not suited to those reservoir characterization problems that are

too complex to be accurately described by simple forward models. For example, the complex molecular interactions that govern NMR relaxation of crude oils cannot be fully described by simple forward models. The present paper is based on a novel application of RBFs for solving inverse problems. This technique was first introduced and demonstrated by Freedman (2006) as a method for solving complex inverse problems for which accurate forward models are unknown. Freedman applied RBFs, *inter alia*, to the prediction of viscosities and molecular compositions of dead oils from NMR measurements.

Let us assume that there exists a database consisting of NMR measurements and live-oil properties at corresponding temperature and pressure conditions. The database measurements for each oil are separated into inputs and outputs. The inputs contain NMR measurements such as T_1 or T_2 distributions, as well as auxiliary measurements including temperature and pressure. The outputs contain the fluid-property to be predicted. The mapping function technique proposes that the underlying physical relationship between database inputs and outputs can be approximated by a mapping function which is a linear combination of Gaussian RBFs. The coefficients of the mapping function are calibrated using the database. The mathematical properties of Gaussian RBFs ensure that the mapping function is unique. The mapping function can be visualized as a multivariate interpolation between database inputs and outputs. For a sample not included in the database, the mapping function can be used to predict the required output from the input measurements made on this sample. The mathematical formulation of the mapping technique is described in the next subsection.

Mathematical Formulation

The notation in this section follows the notation in the Freedman (2006) paper. Let $\vec{f}(\vec{x})$, $\vec{x} \in R^n$ and $\vec{f} \in R^m$ be a real-valued vector function of n variables, and let values of $\vec{f}(\vec{x}_i) = \vec{y}_i$ be given at N distinct points, $\vec{x}_i$, $i = 1,2,\ldots,N$. The values of $\vec{x}_i$ and $\vec{y}_i$ represent the database inputs and outputs, respectively. The interpolation problem is to construct the function $\vec{F}(\vec{x})$ that approximates $\vec{f}(\vec{x})$ and satisfies the interpolation equations,

$$\vec{F}(\vec{x}_i) = \vec{y}_i, i = 1,2,\ldots,N. \quad (1)$$

The interpolation function is constructed as a linear combination of RBFs given as,

$$\vec{F}(\vec{x}) = \sum_{i=1}^{N} \vec{c}_i \varphi(\|\vec{x} - \vec{x}_i\|). \quad (2)$$

The nonlinear functions $\varphi(\|\vec{x} - \vec{x}_i\|)$ are called "radial" because the argument of the function depends only on the distance between, not the direction, of $\vec{x}_i$, from an arbitrary input vector at which the function is to be evaluated. The argument is given by the Euclidean norm in the n-dimensional hyperspace, i.e.,

$$\|\vec{x} - \vec{x}_i\| = \sqrt{\sum_{m=1}^{n} (x_m - x_{i,m})^2}. \quad (3)$$

The forms of commonly used RBFs are listed in Table 1.

The real-valued coefficients $\vec{c}$ of the interpolating function in Equation 2 can be obtained by requiring that the interpolation equations are satisfied exactly. Thus, Equations 1 and 2 imply that the coefficients can be obtained by solving the following linear system of equations,

$$\Phi \cdot C = Y, \quad (4)$$

where C is a matrix whose rows consist of the coefficient vectors i.e.,

$$C = \begin{bmatrix} c_{1,1} & c_{1,2} & \ldots & c_{1,m} \\ c_{2,1} & c_{2,2} & \ldots & c_{2,m} \\ \vdots & \vdots & \vdots & \vdots \\ c_{N,1} & c_{N,2} & \ldots & c_{N,m} \end{bmatrix}. \quad (5)$$

The matrices Φ and Y are $N \times N$ and $N \times m$ matrices, respectively. They contain the RBF and database output vectors and are given by,

$$\Phi = \begin{bmatrix} \varphi_{1,1} & \varphi_{1,2} & \ldots & \varphi_{1,N} \\ \varphi_{2,1} & \varphi_{2,2} & \ldots & \varphi_{2,N} \\ \vdots & \vdots & \vdots & \vdots \\ \varphi_{N,1} & \varphi_{N,2} & \ldots & \varphi_{N,N} \end{bmatrix}, \quad (6)$$

$$Y = \begin{bmatrix} y_{1,1} & y_{1,2} & \ldots & y_{1,m} \\ y_{2,1} & y_{2,2} & \ldots & y_{2,m} \\ \vdots & \vdots & \vdots & \vdots \\ y_{N,1} & y_{N,2} & \ldots & y_{N,m} \end{bmatrix}. \quad (7)$$

Table 1–Forms of commonly used RBFs.

$\varphi(r) = r$	linear
$\varphi(r) = r^2 \log(r)$	thin-plate spline
$\varphi(r) = \exp(-\beta r^2)$	Gaussian
$\varphi(r) = (r^2 + \gamma^2)^{1/2}$	multiquadradics

It can be mathematically proved that the matrix Φ is non-singular for certain functional forms of RBFs such as Gaussian and multiquadrics. This property ensures that the mapping function of Equation 2 is unique. Hence, using a database with N samples, a mapping function that is consistent with the measurements can be uniquely constructed from Equations 2 and 4. For a sample not included in the database, the desired output $\vec{y}$ can be obtained by evaluating the mapping function at the corresponding input $\vec{x}$ i.e.,

$$\vec{y} = \vec{F}(\vec{x}). \tag{8}$$

The mapping function concept is shown pictorially in Fig. 1. The database inputs ($\vec{x}_1$, $\vec{x}_2$,…) are mapped to the corresponding database outputs ($\vec{y}_1$, $\vec{y}_2$,…) using a function $\vec{F}(\vec{x})$. The mapping function is a linear combination of RBFs. The expansion coefficients are uniquely determined such that the interpolation equations (1) are exactly satisfied for N samples in the database. The output $\vec{y}$ for a sample $\vec{x}$ that is not included in the database can be calculated using the mapping function with known coefficients.

Normalized Gaussian RBF

One of the most commonly used RBFs is the normalized Gaussian RBF given as,

$$\varphi(\|\vec{x}-\vec{x}_i\|) = \frac{\exp\left(-\dfrac{\|\vec{x}-\vec{x}_i\|^2}{2s_i^2}\right)}{\displaystyle\sum_{i=1}^{N}\exp\left(-\frac{\|\vec{x}-\vec{x}_i\|^2}{2s_i^2}\right)}. \tag{9}$$

The normalization scales the RBF such that the function value lies between 0 and 1. A Gaussian RBF in two dimensions is shown in Fig. 2. Substituting the expression for normalized Gaussian RBF in Equation 2 the mapping function is given as,

$$\vec{F}(\vec{x}) = \frac{\displaystyle\sum_{i=1}^{N}\vec{c}_i\exp\left(-\frac{\|\vec{x}-\vec{x}_i\|^2}{2s_i^2}\right)}{\displaystyle\sum_{i=1}^{N}\exp\left(-\frac{\|\vec{x}-\vec{x}_i\|^2}{2s_i^2}\right)}. \tag{10}$$

Hence, the mapping function is a linear combination of Gaussian functions whose centers are located at the database inputs.

The widths of the Gaussian RBFs, s_i, determine the topographical behavior of the interpolating function. If the widths are too large ($s_i \to \infty$), then the interpolating function has a flat topography. The function attains a constant value equal to the mean of database outputs as shown here,

$$\lim_{s_i\to\infty}\vec{F}(\vec{x}) = \frac{\displaystyle\sum_{i=1}^{N}\vec{y}_i}{N}. \tag{11}$$

On the other hand, if the widths are too small, the function topography has multiple "hills" and "valleys". Thus, for optimal interpolation, the widths of the Gaussian RBFs are chosen such that they are proportional to the Euclidian nearest-neighbor distances in the input space. This choice ensures that the input space is populated by basis functions that have some overlap with the nearest neighbors and negligible overlap with the more distant ones. The idea is illustrated in a later section in which RBF interpolation is applied for prediction of live-oil properties from NMR measurements.

Physical Interpretation

The physical understanding of RBF interpolation can be obtained by considering the special case in which there is

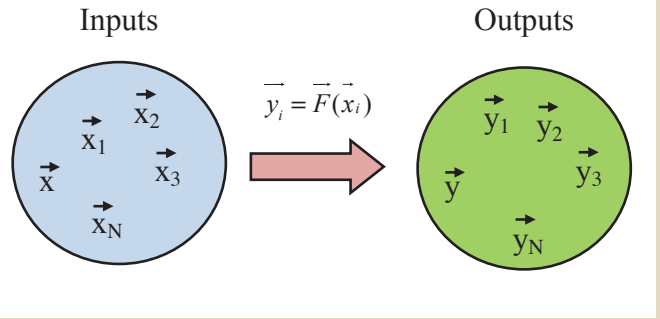

Fig. 1–Pictorial representation of the model-independent mapping function technique. The inputs are mapped to the outputs using a mapping function $\vec{F}$ which is a linear combination of radial basis functions.

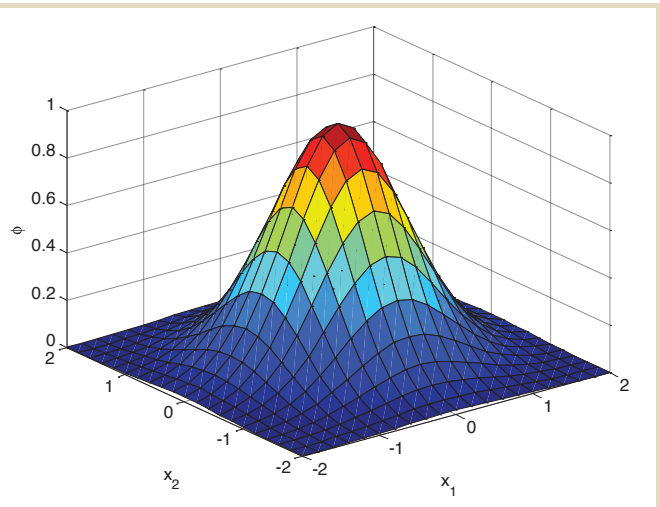

Fig. 2–Gaussian RBF in two dimensions (x_1, x_2) centered at origin.

negligible overlap between Gaussian RBFs. Let us rewrite the interpolation equations, Equation 1, in terms of the mapping function as follows,

$$\vec{F}(\vec{x}_j)=\frac{\vec{c}_j+\sum_{\substack{i=1\\ i\neq j}}^{N}\vec{c}_i\exp\left(-\frac{\left\|\vec{x}_j-\vec{x}_i\right\|^2}{2s_i^2}\right)}{1+\sum_{\substack{i=1\\ i\neq j}}^{N}\exp\left(-\frac{\left\|\vec{x}_j-\vec{x}_i\right\|^2}{2s_i^2}\right)}. \quad (12)$$

If the overlap between RBFs is neglected, the summation in Equation 12 reduces to,

$$\vec{F}(\vec{x}_j)\equiv\vec{y}_j=\vec{c}_j. \quad (13)$$

Substituting Equation 13 in Equation 10 results in the following form of the mapping function,

$$\vec{F}(\vec{x})=\frac{\sum_{i=1}^{N}\vec{y}_i\exp\left(-\frac{\left\|\vec{x}-\vec{x}_i\right\|^2}{2s_i^2}\right)}{\sum_{i=1}^{N}\exp\left(-\frac{\left\|\vec{x}-\vec{x}_i\right\|^2}{2s_i^2}\right)}. \quad (14)$$

Thus, the interpolating function at $\vec{x}$ is the weighted average of the database outputs such that the weights show Gaussian dependence on the proximity of $\vec{x}$ with database inputs. The localized nature of Gaussian functions implies that the mapping function has the largest contribution from the database inputs that are nearest to $\vec{x}$. The database inputs that are far removed from $\vec{x}$ make a negligible contribution to the function.

DATABASE CONSTRUCTION

This section describes the construction of a database consisting of NMR and fluid-property measurements made on live oils at elevated temperature and pressure conditions. The database is used in the subsequent section for prediction of properties of live oils using the mapping technique. Before measurements are performed, each live-oil sample is equilibrated for 1 to 5 days in a pressure cell at a known gas-oil ratio.

NMR Measurements

Acquisition of a database of NMR measurements with live oils was started in 2005 after acquisition of a 2 MHz Maran spectrometer purchased from Resonance Instruments, Inc. A Temco pressure cell, rated to maximum operating conditions of 10,000 psi and 110°C, was installed for high pressure and high temperature measurements. Fig. 3 shows the schematic diagram of the pressure cell. Live oil was charged into the ceramic tube of the sample holder through the ceramic inlet tube. The temperature inside the holder was maintained by circulating Fluorinert through the gap between the ceramic and PEEK tubes as shown in the figure. A second inlet for Fluorinert maintained the pressure through the displacement of the PEEK piston.

Three types of NMR measurements were performed to obtain T_1, T_2, and diffusivity distributions of live oils. T_1 distributions were measured using saturation-recovery pulse sequence. In most cases, joint distributions of T_1 and T_2 were obtained with two-dimensional measurements in which CPMG sequences were preceded by polarization periods with varying wait times. Ten logarithmically spaced wait times were used to measure the T_1 relaxation after saturating the spins with several 90° pulses. T_2 distributions were also obtained using CPMG pulse sequence with a minimal echo spacing of 0.3 ms and a four-step phase cycling. The T_2 values were free of diffusion because the

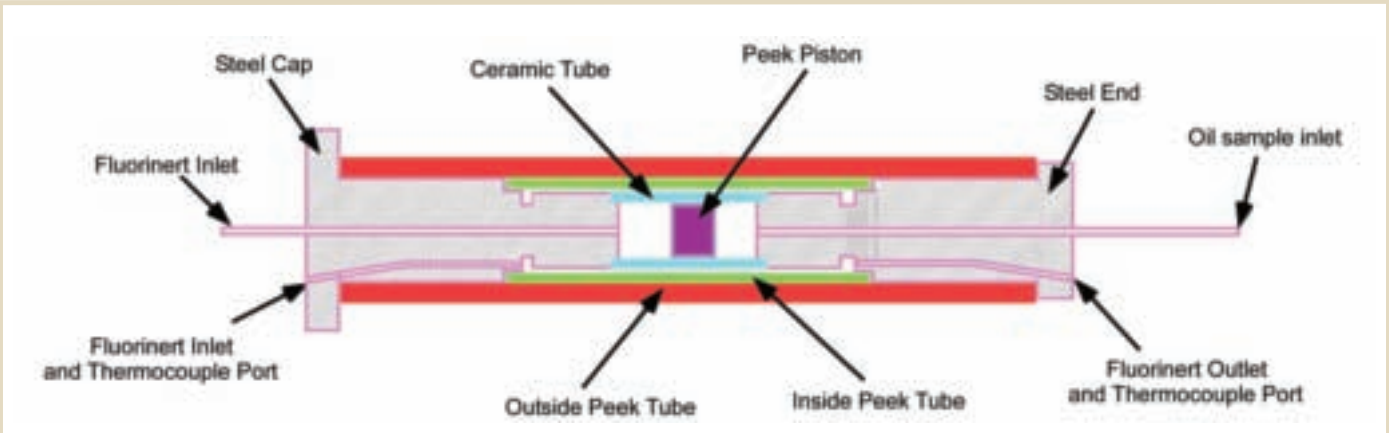

Fig. 3–Schematic of Temco pressure cell. The live-oil samples were maintained above their bubblepoint pressures so that they remain in a single phase.

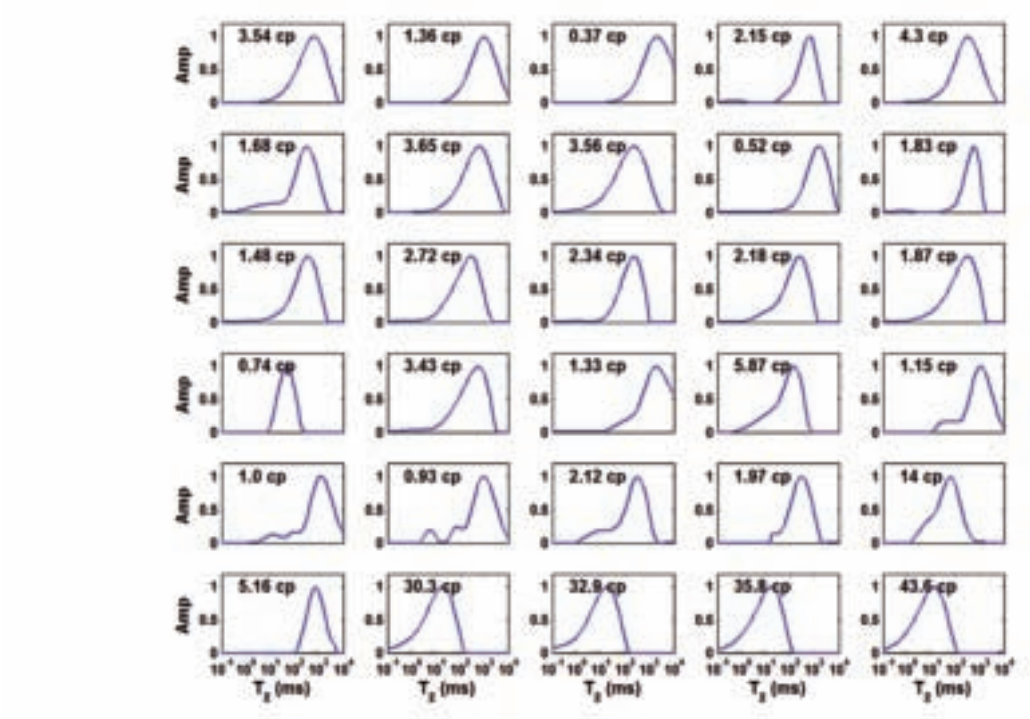

Fig. 4–T_2 distributions of 30 live-oil samples. The viscosities of the samples at corresponding temperature and pressure are also shown.

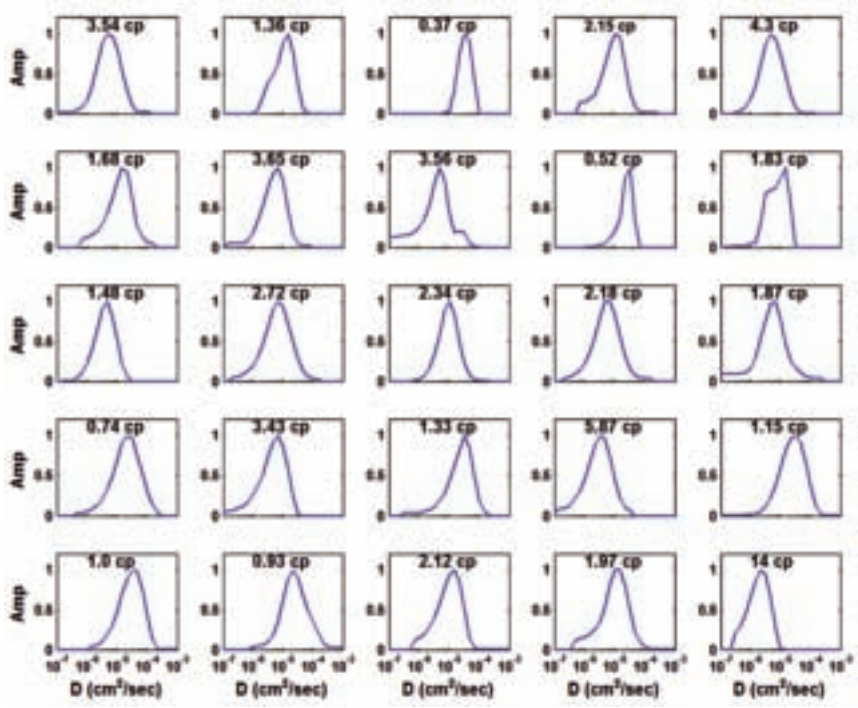

Fig. 5–Diffusion distributions of 25 live-oil samples. The viscosities of the samples at corresponding temperature and pressure are also shown.

spectrometer had no background gradient. Fig. 4 shows the normalized T_2 distributions of 30 live-oil samples in the database. Diffusivity distributions of live oils were obtained using the pulsed-field-gradient pulse sequence. Fig. 5 shows the diffusivity distributions of 25 of the 30 live-oil samples in the database.

Fluid-Property Measurements

The fluid-property measurements on live oils included viscosity, molecular composition, and SARA fraction. Viscosity measurements were made at the same temperature and pressure conditions at which NMR measurements were made. A brief description of the measurements is included below.

Viscosity

An electromagnetic (EM) viscometer was used for measuring viscosity of live oils at elevated temperatures and pressures. The viscosity measurement by an EM viscometer is based on the following principle. A magnetic force is applied to a piston that is immersed in the fluid. The viscous damping force of the fluid on the piston is used to derive an accurate fluid viscosity. Table A1 in Appendix A shows the viscosities and GORs of 30 live-oil samples in the database.

Molecular composition

The molecular composition of live oils in the database was measured using gas chromatography (GC). The weight fraction of components with carbon number ranging from 1 to 30 and higher was obtained by elutriating the fractions with an inert gas. Fig. 6 shows the molecular compositions and corresponding viscosities of 25 live oils for which the diffusivity distributions are shown in Fig. 5.

SARA fraction

The SARA fractions of crude oils were obtained using the standard ASTM technique adopted at Schlumberger DBR Technology Center. The live-oil sample was flashed in an inert nitrogen environment to remove all volatiles from the oil. The flashed oil was separated into asphaltene and maltene fractions by precipitating asphaltenes with an excess of hot heptane. The maltene fractions were further separated into saturates, aromatics, and resins by selective elutriation on activated alumina column. Saturates were elutriated using n-heptane, aromatics using toluene, and resins using equal volumes of dichloromethane and methanol. The weights of each fraction were carefully measured after evaporating the solvent over a hot plate in an inert N_2

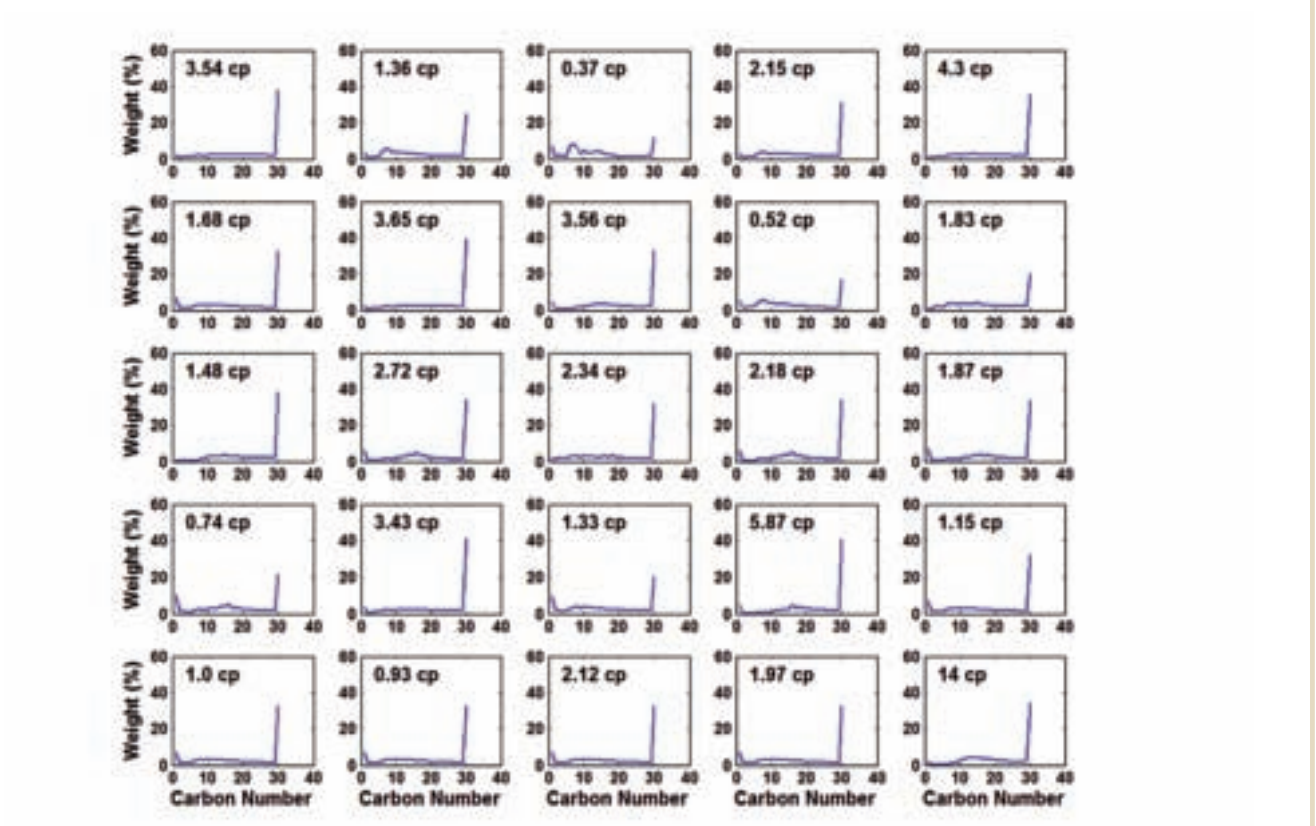

Fig. 6–Molecular composition of 25 live oils measured by GC.

atmosphere. A combined SARA estimate expressed as a weight percentage was obtained from the weights of the fractions. A quality check was done by ensuring that the error in the yield was within 3%.

APPLICATION OF RBF MAPPING

This section describes the application of the RBF mapping technique for estimating live-oil properties using the laboratory database. The mapping technique does not require construction of a physical model, and assumes that the underlying physical relationship between NMR measurements and fluid properties is contained in the database.

Viscosity

NMR relaxation in fluids is sensitive to fluid viscosity due to the dependence of rotational and translational correlation times on the viscosity. The phenomenological BPP theory postulates that in the extreme narrowing limit, the relaxation rate of a pure fluid is proportional to the ratio of fluid viscosity (η) and temperature (T) as shown below,

$$\frac{1}{T_1}=\frac{1}{T_2}\propto\frac{\eta}{T}. \tag{15}$$

The BPP theory assumes that the most significant relaxation mechanism is the intramolecular dipole interactions between nuclei. However, this assumption is not valid for live crude oils because methane molecules relax by different mechanisms compared to larger chain-length hydrocarbons. Lo et al. (2000) developed a mixing rule that correlated the viscosity of mixtures of methane and higher alkanes to the relaxation time, temperature, and gas-oil ratio. This mixing rule assumes that higher alkanes in the mixture relax by intramolecular dipole interactions while methane relaxes by spin rotation and intermolecular interactions. The Lo et al. relationship is given as,

$$\eta=\frac{aT}{T_{2,LM}f(GOR)}, \tag{16}$$

where $T_{2,LM}$ is the logarithmic mean of the T_2 distribution and $f(GOR)$ is an empirically determined function of gas-oil ratio. The parameters for the empirical relationship were obtained from T_2 and viscosity measurements with several methane-alkane mixtures. Equation 16 is frequently employed for prediction of viscosity of live crude oils. However, the accuracy of the predictions is limited for several reasons. First, the viscosity predictions in Equation 16 depend only on the logarithmic mean of the T_2 distributions, i.e., the shapes of the distributions are not taken into account. Second, the effect of pressure on the viscosity of the oils is not explicitly incorporated in the model (Winkler et al., 2004). Third, the empirical constant a needs to be calibrated for different crude oil samples, and the variance in the value can cause significant errors in the predictions. Last, the mixing rule is derived for mixtures of linear alkanes; hence, the proposed relationship may not be valid if nonlinear components are present in the crude oil.

RBF mapping is ideally suited for predicting the viscosity of complex systems such as crude oils from relaxation time or diffusivity distribution. The technique is independent of a physical or empirical model, and incorporates the shape of the distribution in the prediction. Using Equation 10, viscosity can be expressed as a linear combination of Gaussian RBFs whose arguments include the amplitudes of T_2 or D distribution, temperature, pressure, and GOR as shown below,

$$\eta=\frac{\sum_{i=1}^{N}c_i\exp\left(-\frac{\left\|\vec{A}_T-\vec{A}_{T,i}\right\|^2}{2s_i^2}\right)}{\sum_{i=1}^{N}\exp\left(-\frac{\left\|\vec{A}_T-\vec{A}_{T,i}\right\|^2}{2s_i^2}\right)}. \tag{17}$$

Here $\vec{A}_T$ is a vector that contains the amplitudes of T_2 distribution $A(T_2)$ and/or diffusivity distribution $A(D)$, temperature, pressure and GOR of a live-oil sample,

$$\vec{A}_T=\vec{A}_T(A(T_2),A(D),T,P,GOR). \tag{18}$$

The amplitudes of T_2 or D distribution are normalized with the largest respective values to make the inputs dimensionless, and to eliminate the dependence on hardware or software settings. Raw echoes can also be used instead of the amplitudes of T_2 or D distribution since both data contain the same information. In addition, the values of temperature, pressure, and GOR in the input vector are also made dimensionless by normalizing with the respective largest value in the database. The coefficient c is determined from the solution of interpolation equations, Equation 4. The required matrices Φ and Y are obtained using the live oil database of NMR and viscosity measurements. Specifically,

$$\Phi_{i,j}=\frac{\exp\left(-\frac{\left\|\vec{A}_{T,i}-\vec{A}_{T,j}\right\|^2}{2s_j^2}\right)}{\sum_{j=1}^{N}\exp\left(-\frac{\left\|\vec{A}_{T,i}-\vec{A}_{T,j}\right\|^2}{2s_j^2}\right)}1\le i,j\le N, \tag{19}$$

$$y_i=\eta_i, \tag{20}$$

where $\vec{A}_T$ is given by Equation 18 and N is the number of live-oil samples in the database. The viscosity of a live oil not contained in the database can be predicted from Equation 17 using the measured inputs for this sample.

The mapping function of Equation 17 was used for predicting viscosities of live oils using the laboratory database

of the previous section. The input vector for each live oil consisted of normalized amplitudes of T_2 distribution and normalized temperature, pressure, and GOR. The T_2 distribution of live oil 16 was found to be anomalous and thus was not included in the prediction. To ensure sufficient overlap between RBFs, the widths s_j were chosen to be proportional to the Euclidian nearest-neighbor (NN) distances as shown in the following equation,

$$s_j = \alpha (NN)_j, \qquad (21)$$

where the proportionality constant α is of order unity. This choice of the widths of the RBFs ensures that there are at least a few samples in the database that contribute to the mapping function and therefore to the prediction of the fluid properties of an unknown sample. Table A1 in Appendix A lists the NN distances in the input space. In practice, choosing the constant α close to 1 provides accurate predictions, however, a more optimal value of α can be determined by simple trial and error by selecting a value that minimizes the deviation between the measured and predicted values of viscosities. In this case, the optimal α was 1.5. Fig. 7 shows the comparison of predicted live-oil viscosities with the values measured in laboratory. The predictions were obtained using the "leave one out" method whereby one live-oil sample was sequentially removed from the database, and its viscosity was predicted from the interpolating function obtained using the remaining samples. The viscosities are predicted within less than a factor of two for most oils over the entire range.

Viscosities were also predicted using the amplitudes of diffusivity and T_2 distributions as inputs for RBF mapping. Fig. 8 shows the comparison of viscosities of 24 live oils predicted using Equation 17 with the values measured in the laboratory. As mentioned previously, live oil 16 was not included in the prediction. The input vector included normalized amplitudes of T_2 and D distribution, normalized temperature, pressure, and GOR. The widths of RBFs were heuristically determined such that α in Equation 21 was equal to 1.7. The viscosities are predicted within less than a factor of 2 for most cases. A final and important conclusion is that sufficient accuracy can be obtained from a relatively small database of 24 to 30 samples.

Molecular Composition

It is well known that the diffusivity of a spherical molecule suspended in a solvent is inversely proportional to its size. This dependence is clearly elucidated in the Stokes-Einstein relationship,

$$D = \frac{k_B T}{6\pi\eta a_s}, \qquad (22)$$

where a_s is the radius of the diffusing spherical particles, k_B is the Boltzmann's constant, T is the temperature, and η is

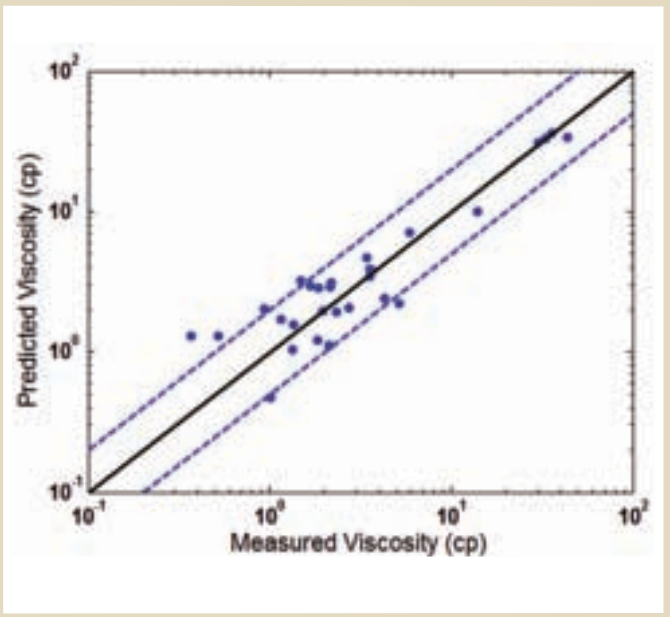

Fig. 7–Comparison of live-oil viscosities predicted from T_2 distributions using the mapping technique with the values measured in the laboratory. The solid black line is the best-fit line and the blue dashed lines are located at the factor of two deviation. In general, the viscosities are predicted within less than a factor of two over the entire range.

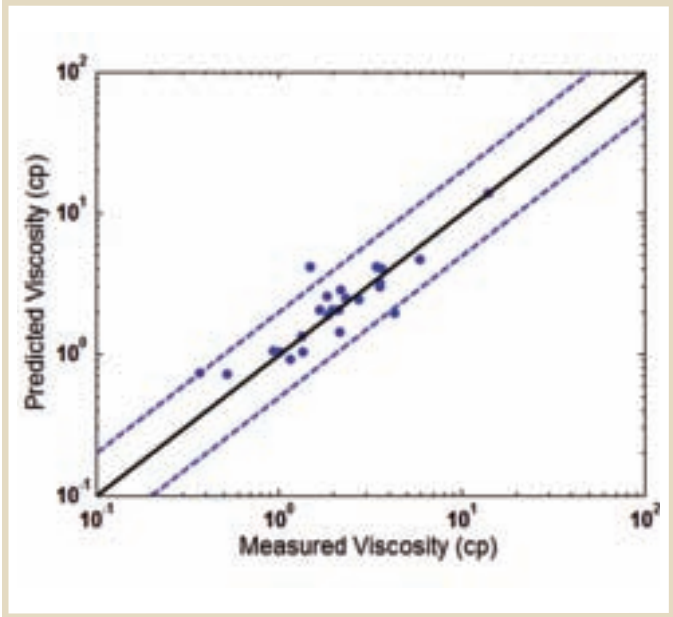

Fig. 8–Comparison of live-oil viscosities predicted from T_2 and diffusivity distributions using the mapping technique with the values measured in the laboratory. The solid black line is the best-fit line and the blue dashed lines are located at the factor of two deviation. In general, the viscosities are predicted within less than a factor of two over the entire range.

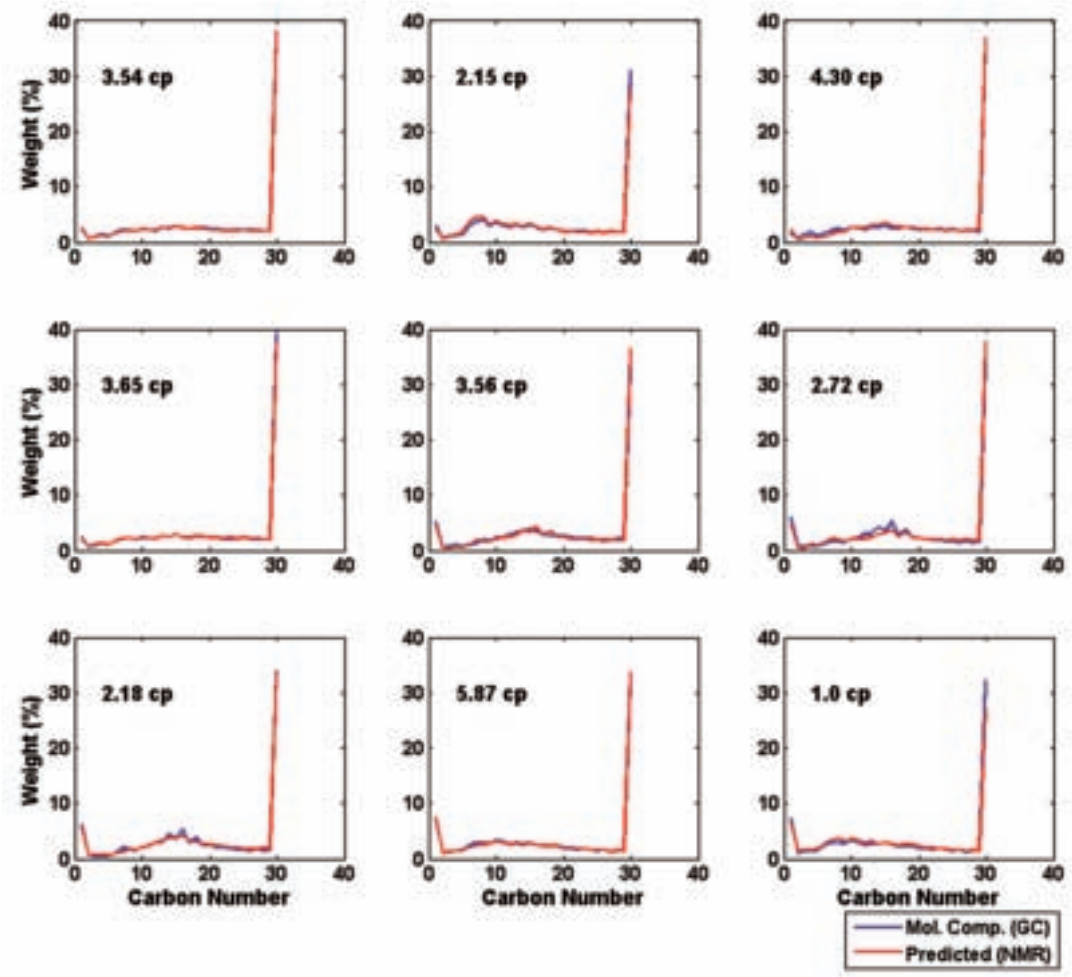

Fig. 9–Comparison of molecular compositions of nine live oils predicted from *D* distribution using the mapping technique with those measured in the lab using GC. Compositions are predicted within 0.5 wt % on average.

the viscosity of the solvent. Equation 22 is strictly valid for hard spheres at dilute concentrations such that the interactions between spheres and the resulting effect on viscosity can be neglected. Similarly, the relaxation time of a molecule is related to its size. Smaller molecules have longer relaxation time, and vice versa. Thus, the molecular composition of a mixture can be predicted from T_2 or D distribution if the interactions between different components can be theoretically modeled.

For molecules with internal degrees of freedom e.g. polymer melts, diffusivity is still related to the size of the molecule; however, Equation 22 is no longer applicable. In linear polymers, diffusivity is found to scale inversely with the number of segments, N_s, as shown below,

$$D \propto N_s^{-\kappa}. \qquad (23)$$

The exponent κ ranges from ½ to 2 depending on whether the hydrodynamic interactions are significant and on entanglement of polymeric chains (Rouse, 1953; Zimm, 1955). Freed et al. (2007) postulated that in a mixture of linear n-alkanes, the diffusivity of a component scales with the chain length as shown here,

$$D_i = N_{s,i}^{-v} g. \qquad (24)$$

The term g is dependent on bulk properties such as viscosity and composition. A similar scaling law between T_2 and chain length was also proposed. Freed et al. applied the physical model to accurately predict the chain-length distribution of dead crude oil samples which had high concentration of paraffins. Another model for predicting the composition of crude oil was proposed by Heaton and Freedman (2005). However, the accuracy of compositions predicted by physical models is limited because the underlying assumptions made in derivation of the models may not be valid for real crude oils. For example, the model developed by Freed et al. (2007) assumes that the crude oil is a mixture of linear alkanes. The presence of components other than

linear alkanes, such as branched hydrocarbons, aromatics, and asphaltenes can influence the accuracy of the physical model.

The mapping technique can be easily applied for predicting molecular compositions from T_2 or D distributions. The multivariate function of Equation 10 maps the database inputs to compositions $\vec{C}_m$ such that the coefficients c are vector quantities of same dimensions as the compositions. Mathematically,

$$\vec{C}_m = \frac{\sum_{i=1}^{N} \vec{c}_i \exp\left(-\frac{\left\|\vec{A}_T - \vec{A}_{T,i}\right\|^2}{2s_i^2}\right)}{\sum_{i=1}^{N} \exp\left(-\frac{\left\|\vec{A}_T - \vec{A}_{T,i}\right\|^2}{2s_i^2}\right)}. \quad (25)$$

The input vector $\vec{A}_T$ consists of amplitudes of T_2 or D distribution, temperature, pressure, and GOR. Similar to the prediction of viscosity, the amplitudes of T_2 or D distribution, temperature, pressure and GOR are normalized to unity with appropriate factors.

The prediction of molecular composition from Equation 25 was tested on the database of 25 live oils. The compositions of these oils were measured in the laboratory using GC. The comparison of the predicted compositions with the measured values is shown in Fig. 9. To save space, the comparison is shown for nine of the live oils in the database. These results are representative of those for the rest of the samples in the database. Compositions were predicted from Equation 25 using normalized amplitudes of D distributions and normalized temperature, pressure, and GOR as inputs. The widths of the RBFs were heuristically determined such that α in Equation 21 was equal to 1, although the predictions were relatively insensitive to values of α from 0.2 to 1. The compositions were predicted using the leave one out method. The average absolute error in the predicted compositions was determined from Equation 26 to be 0.5 wt %,

$$\delta C_m = \frac{1}{N}\sum_{k=1}^{N}\sum_{i=1}^{30}\frac{\left|\vec{C}_{m\,pred}^{\,i,k} - \vec{C}_{m\,meas}^{\,i,k}\right|}{30}, \quad (26)$$

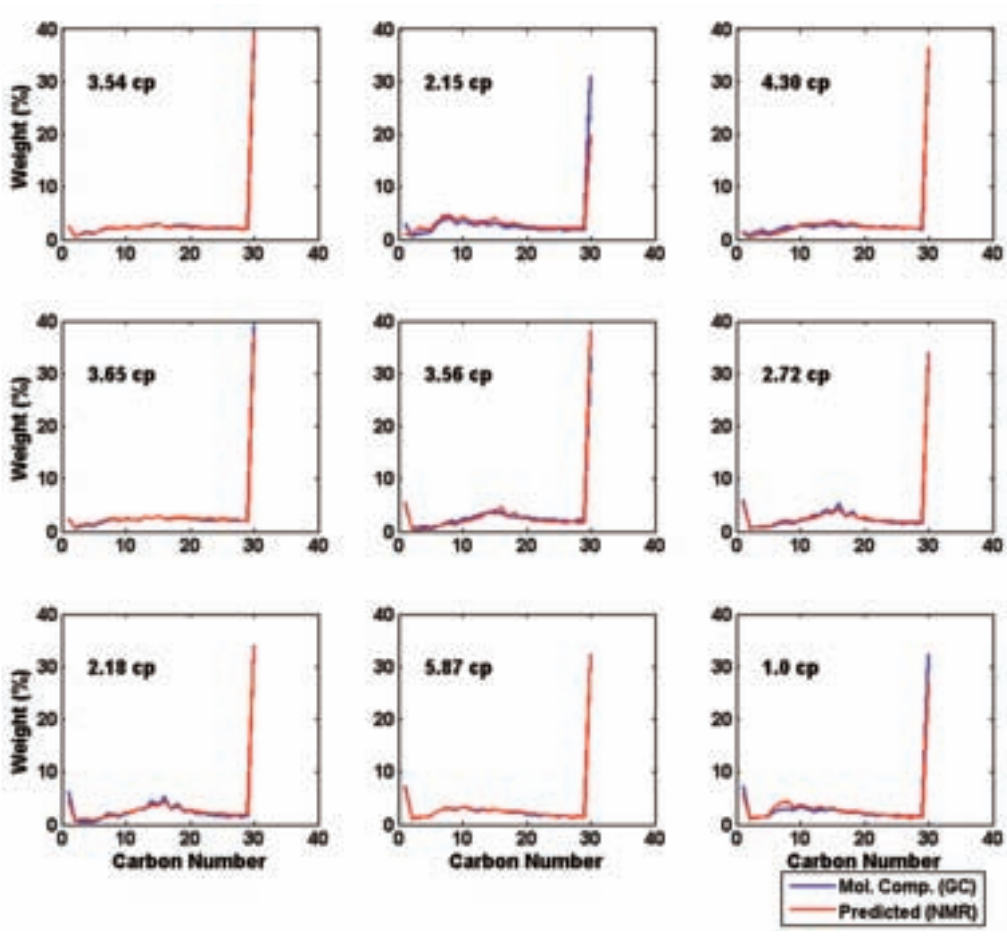

Fig. 10–Comparison of molecular compositions of nine live oils predicted from T_2 and D distribution using the mapping technique with those measured in the lab using GC. Compositions are predicted within 0.5 wt % on average.

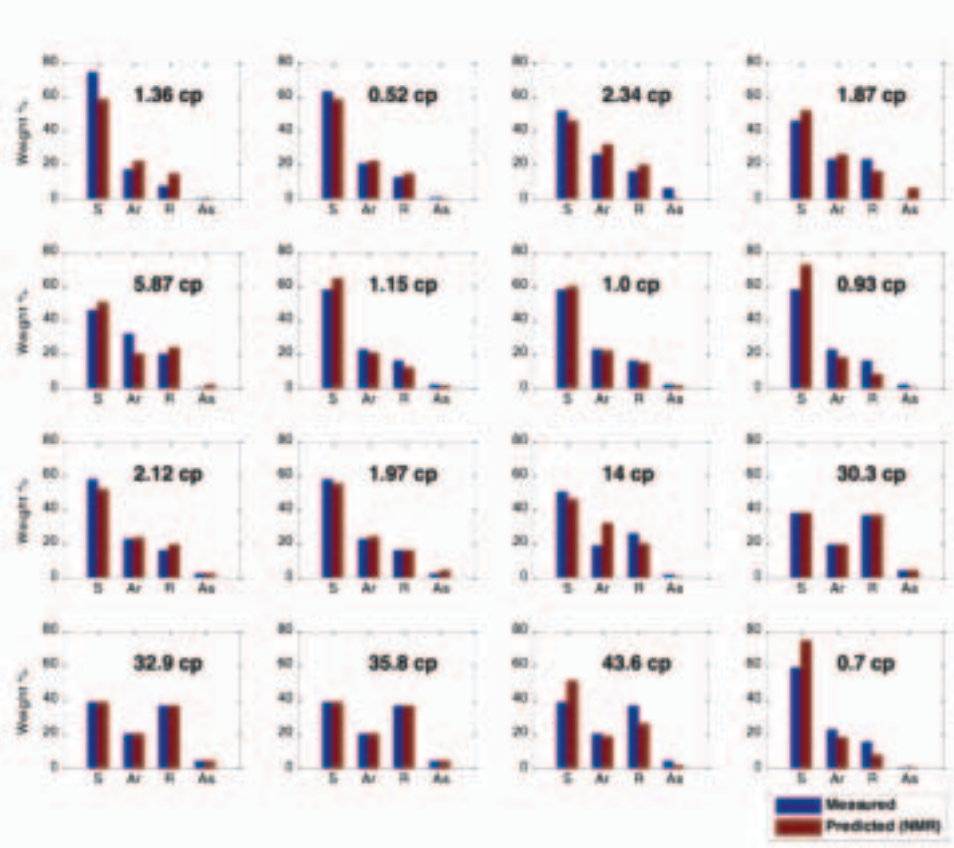

Fig. 11–Comparison of SARA fractions of live oils predicted from RBF mapping with the values measured in the laboratory. SARA fractions are predicted within 13% average absolute deviation.

where $\vec{C}_{m\,pred}$ and $\vec{C}_{m\,meas}$ are the predicted and measured compositions, respectively. The inner sum in the above equation goes over the number of GC components and the outer sum goes over the number of samples in the database.

An excellent correlation between measured and predicted compositions is observed for most oils in the database. The predictions of molecular compositions remain similar for most live oils if GOR is removed from the inputs. This is because the information about the amount of dissolved gas is implicitly contained in the D distributions of live oils. However, for a few live oils, a slight improvement in the accuracy of predicted compositions was observed if GOR was included in the input vector.

Fig. 10 shows the compositions predicted using amplitudes of T_2 and D distributions, temperature, pressure, and GOR as inputs for RBF mapping. The widths were heuristically determined such that α in Equation 21 was equal to 1.0. An excellent agreement between predicted and measured compositions is observed. The accuracy of predicted molecular composition is improved marginally by including the amplitudes of D and T_2 distribution in the input vector.

SARA Fractions

The prediction of SARA fractions of crude oils is important for fluid characterization. SARA analysis helps to provide a consistent basis for comparing oil samples by characterizing the sample according to polarizability (Alboudwarej et al., 2006). SARA fractions are also used to model in-situ combustion, devise flow assurance strategies for prevention of asphaltene deposition, and assess the economics of a potential field development with less uncertainty.

NMR relaxation provides an excellent probe for analyzing different species present in a crude oil. For example, Zhang et al. (2002) found that for heavy oils, T_1/T_2 ratio is correlated to the asphaltene content. Hurlimann et al. (2008) showed that the diffusivity of dead oils with greater than 1% asphaltene content deviates from the established alkane correlation with T_2 relaxation time. This deviation was explained to arise from shortening of crude oil relaxation time in the presence of asphaltenes due to hindered rotational motion of maltene molecules. Additionally, Hurlimann et al. found that the slope of the distributions in D-T_2 domain is correlated to the asphaltene content. However, the results obtained are qualitative.

A quantitative prediction of SARA fractions of live oils can be obtained from NMR measurements using RBF mapping. Analogous to the prediction of molecular composition, SARA content of the oils can be predicted from Equation 10 such that the coefficients c_i are four-dimensional vectors,

$$\overrightarrow{SARA} = \frac{\sum_{i=1}^{N} \vec{c}_i \exp\left(-\frac{\left\|\vec{A}_T - \vec{A}_{T,i}\right\|^2}{2s_i^2}\right)}{\sum_{i=1}^{N} \exp\left(-\frac{\left\|\vec{A}_T - \vec{A}_{T,i}\right\|^2}{2s_i^2}\right)}. \qquad (27)$$

Fig. 11 shows the comparison of SARA fractions predicted from Equation 27 with the laboratory-measured values for 16 live oils in the database. The input vector, $\vec{A}_T$, included normalized amplitudes of T_2 distribution, normalized temperature, pressure, and GOR. The widths were determined such that α in Equation 21 was equal to 0.25. The SARA fractions are predicted within 13% average absolute deviation.

EFFECT OF NOISE ON RBF MAPPING

RBF mapping technique develops a continuous, smooth mapping between database inputs and outputs. As a result, a small variation in the inputs due to uncertainty in measurements or noise in the data leads to only a small variation in the prediction of outputs. This argument can be intuitively understood by recalling that RBF mapping function at $\vec{x}$ is a weighted average of terms that depend on the Euclidean distances of $\vec{x}$ from database inputs. Small errors in measurement of $\vec{x}$ result in minor modifications of the distances, thereby leading to a small variation in the outputs.

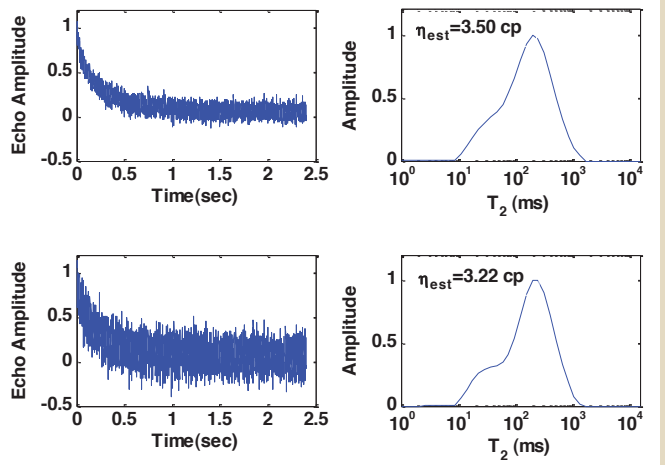

Fig. 12–Effect of noise on the prediction of viscosity using RBF mapping. The upper panel shows the NMR echo data and the corresponding T_2 distribution for live-oil sample 1. The lower panel shows the data with twice the noise and the corresponding T_2 distribution. The RBF viscosity predictions in the two cases change by less than 10%.

The error in RBF predictions due to noise is illustrated by numerical analysis of the variance in the output as a function of noise in the input measurement. For the live-oil sample 1, T_2 distributions at different noise levels were simulated by adding white Gaussian noise to the raw echo data. The resulting distributions were used for predicting the viscosity using the interpolating function of Equation 17. As is shown in Fig. 12, the prediction of viscosity changes by less than 10% even when the noise in T_2 distribution increases by 100%. The analysis shows that the mapping technique is robust and relatively insensitive to the measurement noise. Appendix B derives equations that can be used to estimate the uncertainties in predicted outputs that result from measurement errors.

CONCLUSIONS

The physical and empirical models that relate NMR measurements to crude oil properties have limited accuracy because of the inherent complexity of crude oil systems. A model-independent technique is proposed for predicting properties of live crude oils from NMR measurements. The proposed technique assumes that the underlying physical relationship between NMR response and crude-oil properties is contained in a database of measurements. This relationship is approximated by a mapping function which is a linear combination of Gaussian radial basis functions. The coefficients of the mapping function are uniquely determined such that the function is exactly satisfied for each live-oil sample in the database. Once the coefficients are determined from the database, the mapping function contains no adjustable parameters. For a sample not contained in the database, the desired fluid property can be accurately predicted from the mapping function. A small database of 24 to 30 samples is required for obtaining sufficient accuracy. Numerical analysis shows that the technique is robust in the presence of measurement noise.

It is worth noting that the model-independent technique is applicable for solving any reservoir characterization problem for which a representative database is available.

ACKNOWLEDGEMENTS

The authors would like to thank Dr. Yuesheng Cheng and Dr. Abdel Kharrat at Schlumberger DBR Technology Center for acquiring the live-oil database and Dr. Nick Heaton for constructive comments on an initial version of the manuscript. The authors would also like to thank Schlumberger for the permission to publish the results.

APPENDIX A

Table A1–Viscosities and GOR of 30 live crude oils.

Sample	Temp (K)	Pressure (psia)	GOR (ft^3/STB)	Measured Viscosity (cp)	NN Distance
1	359	5962	275	3.54	0.1013
2	353	8006	381	1.36	0.6438
3	354	6040	885	0.37	0.7384
4	354	8027	339	2.15	0.5332
5	342	6050	232	4.30	0.5266
6	323	5000	763.52	1.68	0.7917
7	359	5564	275	3.65	0.1013
8	355	8045	502	3.56	0.4951
9	366	4893	628	0.52	0.4303
10	351	7891	228.6	1.83	0.5332
11	350	7877	83.17	1.48	0.5266
12	353	10070	598	2.72	0.2921
13	372	7943	271	2.34	0.5463
14	351	9739	563	2.18	0.3835
15	356	9562	742	1.87	0.2921
16	351	10000	1026	0.74	1.3623
17	355	7994	336	3.43	0.5509
18	355	8000	186.31	1.33	0.7384
19	356	9600	467.11	5.87	1.1125
20	362	7500	763.52	1.15	0.3668
21	362	5800	763.52	1.0	0.3668
22	359	4900	763.52	0.93	0.5068
23	322	7800	763.52	2.12	0.4030
24	323	7000	763.52	1.97	0.4557
25	330	5038	161.58	14.0	1.3445
26	353	8048	759	5.16	0.4030
27	343	1700	21.3	30.3	0.1940
28	343	2350	21.3	32.9	0.1805
29	343	3000	21.3	35.8	0.1805
30	343	1400	11.4	43.6	0.3516

APPENDIX B

This Appendix derives some general equations that can be used to compute estimates of the errors in live-oil properties predicted from the RBF mapping function shown in Equation 10. Uncertainties in the predicted live-oil properties will result from errors in the input measurement vector, $\vec{x}$. To make the analysis tractable, we assume that the database measurements are free of errors. This is not a bad assumption since these are typically measured in a laboratory under highly controlled conditions.

The mapping function can be written in the form,

$$\vec{F}(\vec{x})=\frac{\vec{N}(\vec{x})}{D(\vec{x})}, \tag{B1}$$

where we have defined the functions,

$$\vec{N}(\vec{x})=\sum_{i=1}^{N}\vec{c}_i\exp\left(-\frac{\left\|\vec{x}-\vec{x}_i\right\|^2}{2s_i^2}\right), \tag{B2}$$

and

$$D(\vec{x})=\sum_{i=1}^{N}\exp\left(-\frac{\left\|\vec{x}-\vec{x}_i\right\|^2}{2s_i^2}\right). \tag{B3}$$

The variances in the live-oil properties predicted by the RBF mapping function can be written in the form,

$$\vec{\sigma}^2(\vec{F})=\sum_{l=1}^{n}\left(\frac{\partial\vec{F}}{\partial x_l}\right)^2\sigma^2(x_l), \tag{B4}$$

where it has been assumed that the measurements errors are uncorrelated (Freedman and Auburn, 1985). In Equation B4, the $\sigma^2(x_l)$ are the variances (i.e., the square of standard deviations) in the measurements.

Taking partial derivatives in Equation B1 one finds that,

$$\frac{\partial\vec{F}}{\partial x_l}=\frac{D\frac{\partial\vec{N}}{\partial x_l}-\vec{N}\frac{\partial D}{\partial x_l}}{D^2(\vec{x})}, \tag{B5}$$

where the partial derivatives in Equations B4 and B5 are to be evaluated at the input measurement vector. The derivatives in B5 are easily computed and one finds that,

$$\frac{\partial\vec{N}}{\partial x_l}=-\sum_{i=1}^{N}\frac{\vec{c}_i\exp\left(-\frac{\left\|\vec{x}-\vec{x}_i\right\|^2}{2s_i^2}\right)(x_l-x_{i,l})}{s_i^2}, \tag{B6}$$

and

$$\frac{\partial D}{\partial x_l} = -\sum_{i=1}^{N} \frac{\exp\left(-\frac{\left\|\vec{x}-\vec{x}_i\right\|^2}{2s_i^2}\right)(x_l - x_{i,l})}{s_i^2}. \qquad (B7)$$

Equations B4 through B7 can be used to estimate the standard deviations in predicted live-oil properties given estimates of the standard deviations in the measurements.

NOMENCLATURE

Symbol	Description	[Units]
A	Amplitudes of a T_1, T_2, or D distribution	[arbitrary]
$\vec{A}_T$	Concatenated vector containing the inputs for RBF mapping	[arbitrary]
a_s	Radius of the spherical molecule in Equation 22	[m]
$\vec{C}_m$	Molecular composition	[weight %]
δC_m	Average absolute error in the prediction of molecular composition	[dimensionless]
$\vec{c}$	Coefficient vector	
D	Molecular diffusion coefficient	$[cm^2 s^{-1}]$
D_i	Diffusion coefficient of i-th component in Equation 24	$[cm^2 s^{-1}]$
$\vec{f}(\vec{x})$	Multivariate function to be approximated from its sample values	
$\vec{F}(\vec{x})$	RBF approximation to $\vec{f}(\vec{x})$	
$f(GOR)$	Empirically determined function of gas-oil ratio in Equation 16	[dimensionless]
g	Term dependent on crude oil properties in Equation 24	$[cm^2 s^{-1}]$
GOR	Gas-oil ratio	ft^3/STB
k_B	Boltzmann's constant	$[cm^2 g s^{-2} K^{-1}]$
N	Number of samples in database	[dimensionless]
NN	Nearest-neighbor distance in sample space	[dimensionless]
N_s	Number of segments in an alkane molecule	[dimensionless]
P	Pressure of live oil in Equation 18	[psi]
r	Radial distance	[m]
$\overrightarrow{SARA}$	SARA fraction	
s_i	Width of Gaussian RBF centered at database input	[units of $\vec{x}_j$]
T	Temperature	[K]
T_1	Longitudinal relaxation time	[ms]
T_2	Transverse relaxation time	[ms]
$T_{2,LM}$	Logarithmic mean of T_2 distribution	[ms]
$\vec{x}_i$	n-dimensional input vectors in database for i=1,2,…,N	

Greek Symbols	Description	[Units]
α	Proportionality constant in Equation 21	
η	Viscosity	[cp]
η_i	Viscosity of i-th oil in database	[cp]
κ	Exponent of number of segments in Equation 23	[dimensionless]
ν	Exponent of chain length in Equation 24	[dimensionless]
$\varphi(\left\|\vec{x}-\vec{x}_i\right\|)$	RBF centered at $\vec{x}_i$	[dimensionless]
Φ	Interpolation matrix whose elements are RBFs evaluated at the database inputs.	

REFERENCES

Alboudwarej H., Felix, J., Taylor, S., Badry, R., Bremner, C., Brough, B., Skeates, C., Baker, A., Palmer, D., Pattison, K., Beshry, M., Krawchuk, P., Brown, G., Calvo, R., Triana, J. A. C., Hathcock, R., Koerner, K., Hughes, T., Kundu, D., de Cardenas, J. L. and West, C. , 2006, Highlighting heavy oil, Oilfield review, vol. 18, No 2, p. 34-53.

Anand, V., Freedman, R., Crary, S., Minh, C.-C., and Terry, R., 2011, Predicting Effective Permeability to Oil in Sandstone and Carbonate Reservoirs from Well Logging Data, SPE Reservoir Evaluation and Engineering, vol. 14, p. 750-762.

Bloembergen, N., Purcell, E. M. and Pound, R. V., 1948, Relaxation effects in nuclear magnetic absorption, Physical Review, vol. 73, p. 679-712.

Brown, R. J. S., 1961, Proton relaxation in crude oils, Nature, vol. 189, p. 387-388.

Elshahawi, H., Hashem, M., Dong, C., Hegeman, P., Mullins, O. C., Fujisawa, G., Betancourt, S., 2004, Insitu characterization of formation fluid samples – case studies, SPE 90932, Society of Petroleum Engineers, presented at the SPE Annual Technical Conference and Exhibition.

Franke, R., 1982, Scattered data interpolation: test of some methods, Mathematics of Computation, vol. 38, p. 181.

Freed, D., 2007, Dependence on chain length of NMR relaxation times in mixtures of alkanes, Journal of Chemical Physics, vol. 126, p. 174502-1.

Freedman, Robert and Ausburn, Brian, 1985. The Waxman-Smits Equation for Shaly Sands: I. Simple Methods of Solution; II. Error Analysis, The Log Analyst, March-April, p. 11-24.

Freedman, R., 2006, New approach for solving inverse problems encountered in well-logging and geophysical applications, Petrophysics, vol. 47, p. 93-111.

Freedman, R., Anand, V., Zhou, T., Rose, D. and Beekman, S., 2012, A Modern Method for Using Databases to Obtain Accurate Solutions to Complex Reservoir Characterization Problems, SPE Reservoir Evaluation and Engineering, vol. 15, p. 453-461.

Gao, B., Wu, J., Chen, S., Kwak, H. and Funk, J. 2011, New Method for Predicting Capillary Pressure Curves from NMR Data in Carbonate Rocks, SPWLA 52nd Annual Logging Symposium, Paper HH.

Haykin, S., 1999, Neural Networks: A Comprehensive Foundation, Prentice Hall, Hamilton, Ontario, Canada.

Heaton, N. and Freedman, R., 2005, Method for determining molecular properties of hydrocarbon mixtures from NMR data, US Patent 6,859,032.

Hurlimann, M. D., Freed, D. E., Zielinski, L. J., Song, Y. Q., Leu, G., Straley, C., Minh, C, C, and Boyd, A., 2008, Hydrocarbon composition from NMR diffusion and relaxation data, paper U in 49th SPWLA Annual Logging Symposium Transactions: Society of Petrophysicists and Well Log Analysts.

Kansa, E. J., 1990, Multiquadrics – A scattered data approximation scheme with applications to computational fluid dynamics – II, Solutions to parabolic, hyperbolic and elliptic partial differential equations, Computers and Mathematics with Applications, vol. 19, p. 147-161.

Lo, S.-W., Hirasaki, G. J., House, W. V. and Kobayashi, R., 2000, Correlations of NMR relaxation time with viscosity, diffusivity, and gas/oil ratio of methane/hydrocarbon mixtures, SPE 63217, Society of Petroleum Engineers, presented at the SPE Annual Technical Conference and Exhibition.

Micchelli, C. A., 1986, Interpolation of scattered data: distance matrices and conditionally positive definite functions, Constructive Approximation, vol. 2, p. 11-22.

Okuyig, M., Berrim, A., Xian, C. and Haddad, S., 2007, Continuous downhole fluid log powered by an integrated approach reveals reservoir fluid complexities and minimizes uncertainties, SPE 109539, Society of Petroleum Engineers, presented at the SPE Asia Pacific Oil and Gas Conference and Exhibition.

Ratulowski, J., Amin, A., Hammami, A., Muhammad, M. M. and Riding, M., 2004, Flow assurance and subsea productivity: Closing the loop with connectivity and measurements, SPE 90244, Society of Petroleum Engineers, presented at the SPE Annual Technical Conference and Exhibition.

Rouse, P. E., 1953, A Theory of the linear viscoelastic properties of dilute solutions of coiling polymers, Journal of Chemical Physics, vol. 21, p. 1272-1280.

Tarantola, A., 2005, Inverse Problem Theory: Methods for Data Fitting and Methods for Model Parameter Estimation: SIAM books, Philadelphia, PA.

Winkler, M., Freeman, J. J. and Appel, M., 2004, The limits of fluid property correlations used in NMR well logging: An experimental study of reservoir fluids at reservoir conditions, paper DD in 45th SPWLA Annual Logging Symposium Transactions: Society of Petrophysicists and Well Log Analysts.

Zhang, Y., Hirasaki, G. J., House, W. V. and Kobayashi, R., 2002, Oil and gas NMR properties: The light and heavy ends, paper HHH in 43rd SPWLA Annual Logging Symposium Transactions: Society of Petrophysicists and Well Log Analysts.

Zimm, B. H., 1955, Dynamics of polymer molecules in dilute solution: Viscoelasticity, flow birefringence and dielectric loss, Journal of Chemical Physics, vol. 24, p. 269-278.

ABOUT THE AUTHORS

Vivek Anand is a Senior Research Scientist at Schlumberger Sugar Land product center. Vivek obtained a Bachelor of Science degree from Indian Institute of Technology, New Delhi in 2002 and a PhD from Rice University, Houston in 2007, both in Chemical Engineering. At Schlumberger, his research interests include NMR in porous media, fluid characterization, and mathematical modeling. He was a SPWLA distinguished speaker in 2009, the recipient of best paper award at the 2005 SPWLA annual symposium and of the 2011 SPE Young Professional best paper award.

Dr. Bob Freedman is a Scientific Advisor at the Schlumberger Houston Pressure and Sampling Center. Bob has worked for Schlumberger for 26 years and is recognized worldwide in the industry for his wide ranging and significant technical achievements. Prior to joining Schlumberger, Bob worked for five years in operations and research for Shell and five years as an independent formation evaluation consultant. During his 36 year industry career he has published more than 40 SPE, SEG, and SPWLA papers and has been granted more than 30 patents on well logging technology. Bob has been active in both the SPE and SPWLA having served as a Distinguished Lecturer for both organizations and also as a Distinguished SPE Author. Bob served as VP of Technology for SPWLA in 2008. He received a 2009 SPWLA Award for Distinguished Technical Achievement and the 2004 SPE Cedric Ferguson Certificate.